ELSEVIER

S0032-3861(96)00452-1

Polymer Vol. 37 No. 26, pp. 5917–5925, 1996

0032-3861/96/$15.00 + 0.00

Porous polymeric membranes by bicontinuous microemulsion polymerization: effect of anionic and cationic surfactants

T. H. Chieng, L. M. Gan* and W. K. Teo†
*Department of Chemical Engineering and *Department of Chemistry, National University of Singapore, Singapore 119260, Republic of Singapore*

and K. L. Pey
Institute of Microelectronics, 11 Science Park Road, Singapore Science Park II, Singapore 117685, Republic of Singapore
(Received 21 February 1996; revised 27 March 1996)

Porous polymeric membranes made by polymerizing bicontinuous microemulsions stabilized with anionic sodium dodecyl sulfate (SDS) and cationic dodecyltrimethylammonium bromide (DTAB) as surface-active agents were investigated. The morphology, swelling and permeability characteristics of the membranes were found to be highly dependent on the surfactant concentration in both SDS and DTAB systems. The pore size of the DTAB system decreases on increasing the DTAB concentration, while the reverse trend was observed for the SDS system until its concentration exceeded 10 wt%. The membrane prepared using SDS was found to have a larger pore size in the range of 100 nm to 3 μm as compared to that of DTAB, which is less than 100 nm. In addition, the variation of SDS concentration led to a continuous change in the shape of particle aggregates of the membranes while it appeared to remain in globular form for the DTAB system. The remarkable differences between the membranes prepared using SDS and DTAB are discussed in terms of their different monolayer flexibilities. Copyright © 1996 Elsevier Science Ltd.

(Keywords: microemulsions; bicontinuous; porous)

INTRODUCTION

Porous membranes were produced by various methods using phase inversion process[1,2], emulsion polymerization[3,4] and most recently microemulsion polymerization[5–17]. Much work has been done based on the first two methods while the research carried out on microemulsion polymerization is still limited. Control of pore size and pore size distribution have been emphasized, especially in the phase inversion process to obtain selective permeable membranes. It is known that the precise control of the pore size of membranes is difficult. This is because even a slight fluctuation of the processing conditions might result in a membrane with a broad pore size distribution. To our knowledge the preparation of polymer, in thin film or membrane form, from microemulsion polymerization for characterization is still rather limited.

In our previous studies[14–16], polymeric materials consisting of coagulated aggregates with open-cell structures could be obtained by polymerization of monomer(s)-containing bicontinuous microemulsions. In this paper, our aim is to present a comparative study on the porous polymeric membranes from bicontinuous microemulsions using both anionic sodium dodecyl sulfate (SDS) and cationic dodecytrimethyl ammonium bromide (DTAB) as surface-active agents.

† To whom correspondence should be addressed

EXPERIMENTAL

Materials

Methyl methacrylate (MMA) from BDH, 2-hydroxyethyl methacrylate (HEMA) and ethylene glycol dimethacrylate (EGDMA) from Merck were purified under reduced pressure before use. The redox initiator consisting of $N,N,N'N'$-tetramethylethylene diamine (TMEDA) and ammonium persulfate (APS), of purity greater than 99% and 98%, was used as received from Aldrich. SDS of purity greater than 99% was used as received from Fluka. DTAB of purity greater than 98% was recrystallized from acetone–ethanol mixture (3/1, v/v) before use. Water used was purified by a Milli Q water system with conductivity *ca* 1 μS cm^{-1}.

Phase diagram

The clear regions of the microemulsion systems consisting of MMA, HEMA and water using either anionic SDS (system I) or cationic DTAB (system II) were determined visually at room temperature (30°C). MMA, HEMA and EGDMA of known proportions

Table 1 Bicontinuous microemulsion compositions used for preparing membranes

Membrane[a]	Composition (wt%)					Appearance[b]	
	SDS	DTAB	MMA	HEMA	Water	BP	AP
S10	4	–	18	42	36	C	O
S15	6	–	18	42	34	C	O
S20	8	–	18	42	32	C	O
S25	10	–	18	42	30	C	O
D17	–	6.8	18	42	33.2	B	WY
D20	–	8	18	42	32	C	BY
D25	–	10	18	42	30	C	LB
D30	–	12	18	42	28	C	C

[a] MMA/HEMA weight ratio was fixed at 30/70. EGDMA added was 4.0 wt% based on the total weight of MMA and HEMA, while APS was 0.3 wt% based on the total weight of the aqueous phase. TMEDA added was 2 drops per 5.0 g of each microemulsion sample. The amount of aqueous solution of SDS or DTAB was maintained at 40 wt%

[b] BP, before polymerization; AP, after polymerization; C, clear; O, opaque; WY, white yellowish; B, bluish tinge; BY, bluish yellow; LB, light blue

Note: the numbers after each symbol denote the weight percent of SDS or DTAB in water for each microemulsion sample

were mixed thoroughly in culture tubes before they were titrated with a stock solution containing either 20 wt% SDS or 20 wt% DTAB in water. EGDMA added was 4 wt% based on the total weight of MMA and HEMA.

Preparation of bicontinuous microemulsions

Table 1 lists the bicontinuous microemulsion compositions used to prepare membranes. The aqueous component of each microemulsion sample was fixed at >20 wt% in order to give a comparable amount of oil and aqueous domains, which is a requirement for a bicontinuous microemulsion. Besides, it has also been established in our previous studies[13–16] and those reported by others[10–12] that microemulsion compositions having water content greater than 20 wt% show the existence of bicontinuous structures. EGDMA added in each sample was 4.0 wt% based on the total weight of MMA and HEMA.

Preparation of the membrane

A reactive redox initiator[18] consisting of TMEDA/APS was used for polymerization in this study. The amount of APS used was 0.3 wt% (13.1 mmol l^{-1}) based on the total weight of the aqueous phase, while two drops TMEDA per 5.0 g of each microemulsion sample were added. The polymerization was carried out at 25°C in an anaerobic chamber filled with nitrogen gas for 6 h. The prepared bicontinuous microemulsions were allowed to polymerize for 1–2 min before they were transferred in between two well-cleaned and dried glass plates (12 × 10 cm) and squeezed slowly to avoid trapping of air bubbles. The thickness of the membrane in the dry form, in the range of 0.08–0.12 mm, was measured accurately with a palmer. The dried membrane was brittle at room temperature, and became softer in a high humidity environment. The membranes obtained were leached in hot water at 50°C until the conductivity of the effluent was similar to that of pure water in order to remove the surfactants and perhaps some unpolymerized monomers. This was reconfirmed by elemental analyses which indicated that no detectable SDS or DTAB remained.

Degree of swelling

After the membrane was completely dried *in vacuo* at room temperature until a constant weight was attained, the dried membrane, weight W_a, was immersed in water at 25°C until the swelling equilibrium was reached. The swollen membrane was then weighed after blotting free surface water.

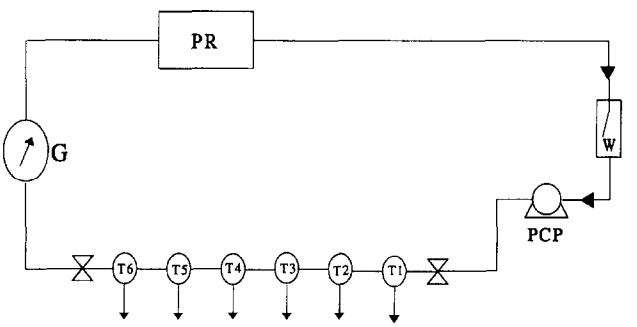

Figure 1 A schematic diagram of a liquid membrane test cell. PCP, pressure control pump; T_i ($i = 1-6$), membrane test cell; G, pressure gauge; PR, pressure regulator; W, water reservoir. The arrows marked in the figure show the direction of water flow

The degree of swelling, equilibrium water contents (*EWC*), for the membranes was defined as:

$$EWC(\%) = \frac{W_s - W_d}{W_s} \times 100 \qquad (1)$$

where W_s and W_d denote the weight of the water swollen membrane and the dry membrane respectively.

Sorption kinetics of the membrane

For sorption kinetic studies, each membrane disk of diameter 2.0 cm and known thickness, was immersed in millipore water at 25°C and rapidly removed from the water at various times, wiped off with tissue paper to remove the surface adherent water and weighed.

Water permeability through membranes

The porous polymeric membranes, of which swelling equilibrium in pure water at 25°C was attained, was used for the water permeability study. The apparatus used for this study is schematically shown in *Figure 1*. Experiments were carried out at 25°C under an operating pressure of 150 psi (10.2 atm). The permeability coefficients (K) of

Table 2 Water sorption characteristics parameters of the membranes

Membrane[a]	*EWC* (%)	$10^7 D$ ($cm^2 s^{-1}$)	$10^6 P_w$ [b] ($mol\,h^{-1}\,cm^{-1}\,atm^{-1}$)	$10^{16} K$ [c] (cm^4)
S10	35.2	1.17	3.73	17.8
S15	34.1	1.89	1.53	7.34
S20	36.3	19.2	60.1	288
S25[d]	35.6	34.8	–	–
D17	23.2	0.38	0.071	0.340
D20	20.6	0.45	0.014	0.069
D25	18.5	0.59	8.07	38.6
D30	16.9	0.40	0.015	0.070

[a] The membranes were prepared from bicontinuous microemulsion compositions as shown in *Table 1*
[b] $P_w = Jt/A\Delta P$
[c] $K = Jt\eta/\Delta P$
[d] The water permeability coefficient of the membrane S25 was not performed due to its fragility
A, Effective filtration area (cm^2); *J*, flow rate ($mol\,h^{-1}$ or $cm^3\,s^{-1}$); P_w hydraulic permeability coefficient ($mol\,h^{-1}\,cm^{-1}\,atm^{-1}$); K, permeability coefficient (cm^4); *t*, thickness of membrane (cm); ΔP, difference in pressure (atm or dyn cm^{-2}); η, viscosity of water (dyn s cm^{-2})

pure water through the membranes are summarized in *Table 2*. For convenience of comparison with other papers, the hydraulic permeability coefficients[19,20] P_w are also shown.

Electron microscopic investigation

A Hitachi S-4100 field emission scanning electron microscope (FESEM) was used to examine the morphology of the resulting polymeric membranes. For the cross-section view of the membranes, the membranes were freeze-fractured in liquid nitrogen, while for the surface morphology, they were used directly for examination. Prior to examination, all the samples were vacuum dried at room temperature for 24 h, before coating with a thin layer of gold using a JEOL ion-sputter JFC-1100 coating machine.

RESULTS

Phase diagram

The microemulsion phase diagram for the system MMA/HEMA/water containing either 20 wt% SDS (system I) or 20 wt% DTAB aqueous solution (system II) is shown in *Figure 2*. A large single-phase transparent microemulsion region resembling that of Winsor IV[21] extended from the water-rich apex to the MMA-rich apex, and a multi-phase region D was obtained for each of the SDS and DTAB systems. However, it appeared that system II using DTAB showed a smaller microemulsion region at aqueous solution content in the range of *ca* 5–40 wt%. At aqueous content greater than 40 wt%, system II behaved in the reverse manner, that is, it showed a slightly larger microemulsion region as compared to that of system II using SDS. The rough demarcation on the phase diagram was based on our previous studies on similar systems[14,15]. At low aqueous content, as represented by region A, it is believed that water-in-oil (W/O) droplet structures exist while at high aqueous content (region B), oil-in-water (O/W) droplet structures exist. At intermediate aqueous content (region C), bicontinuous structures prevail.

Polymerizations

Table 1 shows the various bicontinuous microemulsion

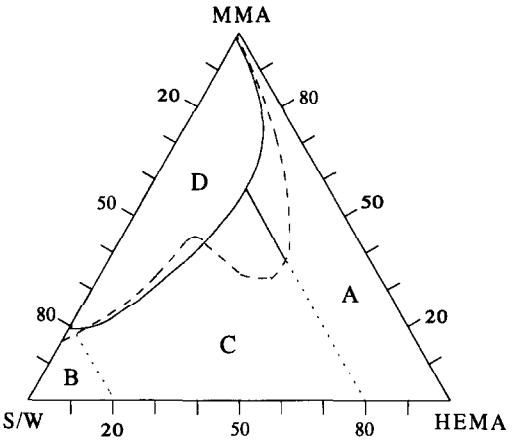

Figure 2 Phase diagram of the microemulsion systems consisting of MMA, HEMA and water using anionic SDS and cationic DTAB as surface-active agents. EGDMA added was 4 wt% based on the total weight of MMA and HEMA. The amount of SDS or DTAB was 20 wt% in water. Symbol S/W represents surfactant (either SDS or DTAB)/water. Domains: A, W/O microemulsion; B, O/W microemulsion; C, bicontinuous microemulsion; D, multiphase region. ——, SDS system, – – – –, DTAB system

compositions formulated with either anionic SDS or cationic DTAB as the surface-active agents. For the microemulsion system using SDS, the amount of surfactant needed to stabilize the system at a particular composition was ~ 1.5 wt%, while ~ 7.0 wt% was required to maintain the transparency of the microemulsions for the system using DTAB. In both systems, the gelation of the microemulsion samples starts within 5 min. The redox initiator, APS/TMEDA, was chosen because the polymerization could be carried out at a relatively low temperature, so as to minimize the occurrence of phase separation as well as evaporation of monomers. In addition, this particular redox system has been found[18] to give a rapid polymerization rate.

After polymerization the microemulsion samples using SDS transformed into final opaque polymeric membranes. No noticeable changes in appearance were observed on increasing the SDS concentration. However, on further increase of SDS concentration beyond 10 wt%, severe phase separation ocurred through precipitation of polymers which were insoluble in the system which leads to the formation of membranes with low mechanical strength and high fragility. This process occurred before the onset of gelation. On the contrary, the opacity of the membranes seemed to decrease on increasing the surfactant concentration for DTAB system.

Microstructure of polymeric membranes

The effect of SDS concentration on the microstructure of the porous polymeric membranes is illustrated in *Figures 3a*, *3b*, *3c* and *3d*, for samples S10, S15, S20 and S25 respectively. *Figures 3a(i)*, *3b(i)*, *3c(i)*, and *3d(i)* show the morphology of the surface of the membranes which were in direct contact with the glass plates, while *Figures 3a(ii)*, *3b(ii)*, *3c(ii)* and *3d(ii)* represent the cross-sectional view of the membranes. *Figures 3a(iii)*, *3b(iii)*, *3c(iii)* and *3d(iii)* depict the cross-sectional view at a higher magnification in order to give a better understanding of their morphologies, especially the skin layer of the membranes. As observed from the

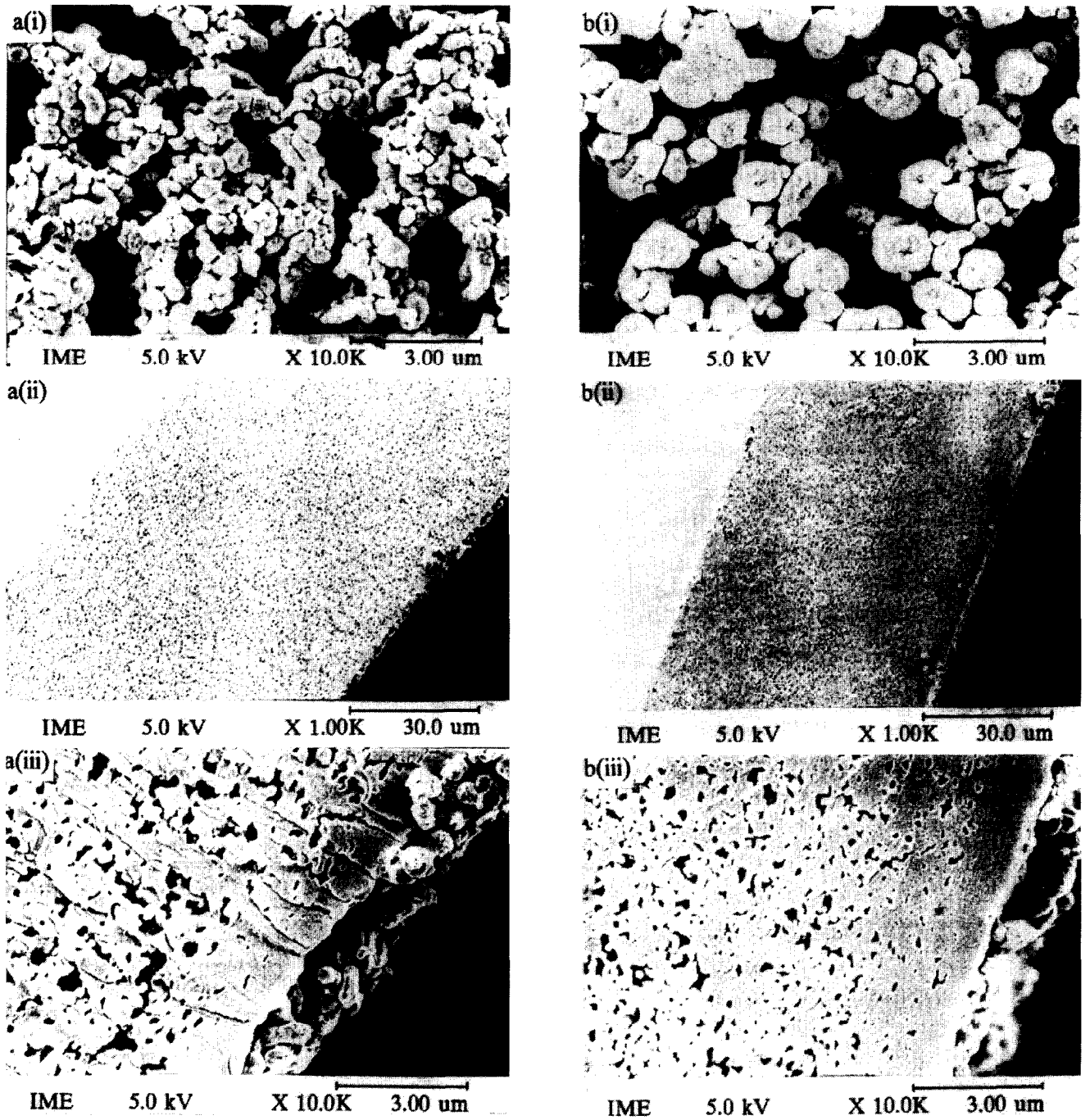

Figure 3 FESEM micrographs of the porous polymeric membranes. (a) S10; (b) S15; (c) S20; (d) S25. (i) Surface in direct contact with the glass plate; (ii) cross-sectional view of the membrane; (iii) cross-sectional view close to the skin layer of the membranes at a high magnification

micrograph (*Figure 3a(i)*) for sample S10 which contained 4 wt% SDS, globular aggregates of dimension *ca* 0.1–0.5 μm which were coagulated with elongated aggregates of dimension *ca* 0.5 μm in width and 1–2 μm in length were obtained. When the SDS concentration was increased further, as for sample S15 (*Figure 3b(i)*), the polymer aggregates became elliptical rather than globular or elongated in shape, with a depression in the middle portion of the particles. They were *ca* 0.6–1.0 μm in width and 0.8–1.5 μm in length. The elliptical polymer aggregates as observed for sample S15 became more spherical in shape when SDS concentration was increased to 8 wt% as illustrated in *Figure 3c(i)*. On increasing the SDS concentration to 10 wt% (sample S25), only globular polymer particles coagulated with each other were observed, as shown in *Figure 3d(i)*. The globular structures were *ca* 0.1–0.3 μm in diameter. The size of the aggregates seemed to decrease drastically when the SDS concentration was increased from 8 to 10 wt%. The results show that the particle morphology strongly depends on the SDS concentration in the precursor bicontinuous microemulsions. On their cross-sectional view, it was observed that the pores of the membranes were randomly distributed and sponge-like in structure, similar to the structure of the channels of the bicontinuous microemulsions as observed using the technique of freeze fracture transmission electron microscopy (FFTEM)[22,23] and those models predicted

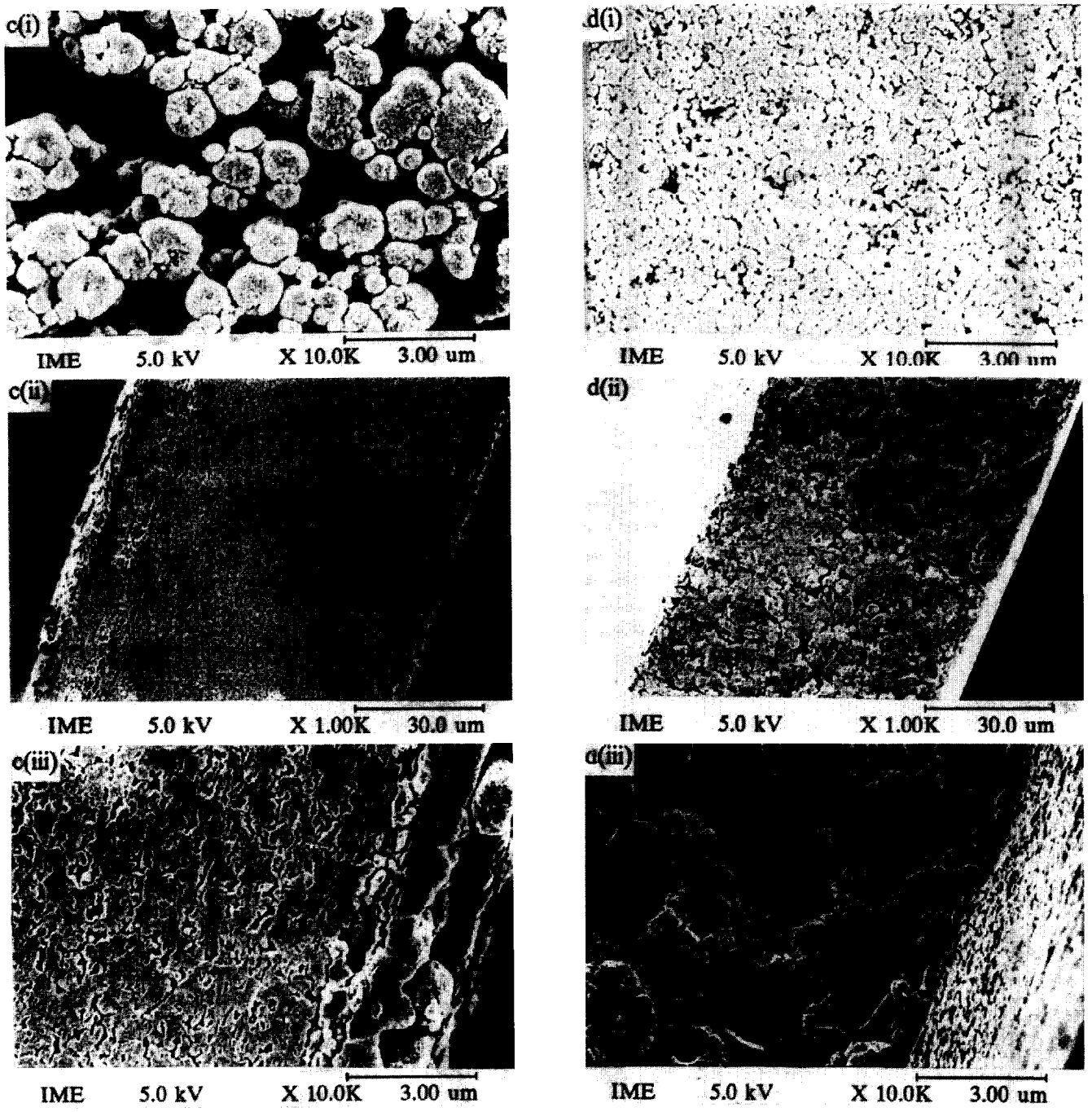

Figure 3 (*Continued*)

by several authors[24–26]. The pore sizes were in the range of *ca* 200–800 nm for sample S10 (*Figure 3a(ii)*), *ca* 100–300 nm for both samples S15 (*Figure 3b(ii)*) and S20 (*Figure 3c(ii)*) and 1–3 μm for sample S25 (*Figure 3d(ii)*). These pore sizes were still too large as compared to that of the typical width of bicontinuous structures (60–80 nm) as reported in the literature[22,23].

Figures 4a, *4b*, *4c* and *4d* show the morphology of the porous polymeric membranes for samples D17, D20, D25 and D30 respectively, using DTAB as the surfactant. In contrast to those samples using SDS, the morphology of the membranes using DTAB appeared to consist of coagulated spherical aggregates only, with the size of the aggregates decreasing on increase of the DTAB concentration for samples D17, D20, D25 and D30, as depicted in *Figures 4a(i)*, *4b(i)*, *4c(i)* and *4d(i)* respectively. The globular aggregates were decreased from *ca* 0.15–0.4 μm for sample D17 (contains 6.8 wt% DTAB) to *ca* 0.05–0.15 μm for sample D30 (contains 12 wt% DTAB). Micrographs clearly indicate the closer packing of the polymer particles on increasing the DTAB concentration. The pore sizes for samples D17 (*Figure 4a(ii)*) and D20 (*Figure 4b(ii)*) were *ca* 50–100 nm and 20–60 nm respectively, and further decreased to below 20 nm, as for samples D25 (*Figures 4c(ii)*) and D30 (*Figure 4d(ii)*), which were rather difficult to discern from FESEM micrographs due to coating effect. However, it was noted that the globular aggregates were very well-defined for sample D25 as compared to

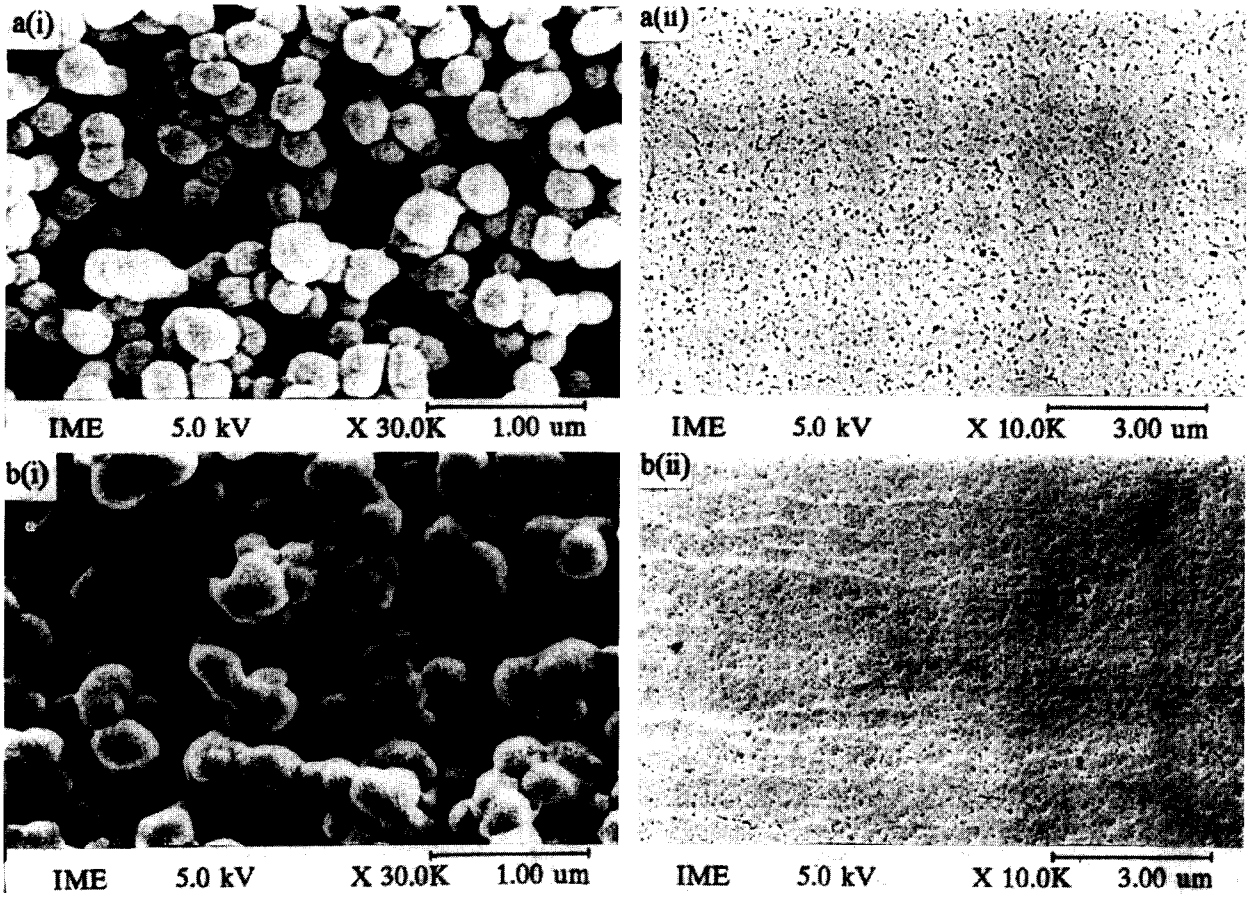

Figure 4 FESEM micrographs of the porous polymeric membranes. (a) D17; (b) D20; (c) D25; (d) D30. (i) Surface in direct contact with the glass plate; (ii) cross-sectional view of the membrane. (c) (iii) and (d) (iii) show the cross-sectional view closed to the skin layer of the membranes at a high magnification

other samples containing lower or higher DTAB concentration than 10 wt%. The smaller aggregated sizes for system using DTAB are also responsible for the higher optical transparency compared to those systems using SDS.

Swelling equilibria

A remarkable difference in swelling equilibrium was observed for the membranes made with anionic and cationic surfactants. *EWC* for system I using SDS remained almost constant on increasing the SDS concentration, as illustrated in *Figure 5*. On the contrary, a decrease in *EWC* values for DTAB system was observed on increasing the surfactant concentration. In addition, higher *EWC* values were obtained for system I, compared to those of system II.

Sorption kinetics

The reduced sorption curves, M_t/M_∞ *versus* $(t/L^2)^{0.5}$ of the membranes for SDS and DTAB systems are given in *Figures 6* and *7* respectively; M_t is the amount of water sorbed in time t and M_∞ is the corresponding limiting value at equilibrium; L is the thickness of the dry film, presumed constant over the whole sorption process. The average diffusion coefficient (D) of water within the polymer matrix, measured in the sorption mode may be derived directly from the initial slope according to the following well-known equation[27]:

$$\frac{d(M_t/M_\infty)}{d[(tL^{-2})^{0.5}]_{t\to 0}} = 4\left(\frac{D}{\pi}\right)^{0.5} \quad (2)$$

The calculated D values are given in *Table 2*. An increase in D was observed on increasing the surfactant concentration for the SDS system, while there seemed to be no appreciable variation in D for the DTAB system. The reduced sorption curves for SDS system were very different from those of the DTAB system. For the SDS system, the curves showed an initial sharp linear increment followed by a gradual increment before levelling off, while for the DTAB system, the curves resembled an S-shape, with an initial linear increase, followed by a sudden increase and then finally levelling off.

Water permeability through the membranes

The permeability coefficient (K) of pure water through the membranes at 25°C under an operating pressure of 150 psi (10.2 atm) are summarized in *Table 2*. The water permeability was relatively low for membranes prepared from precursor bicontinuous microemulsions containing low and high surfactant concentration for both systems. For the SDS system, the highest water permeability was observed when 8 wt% SDS was used, whereas the corresponding value was 10 wt% for the DTAB system.

DISCUSSION

It has been found[28] that short chain alcohols can be added to the microemulsions so as to lower the rigidity of the interfacial film. In this study, HEMA which possesses the same characteristics as these alcohols, is incorporated

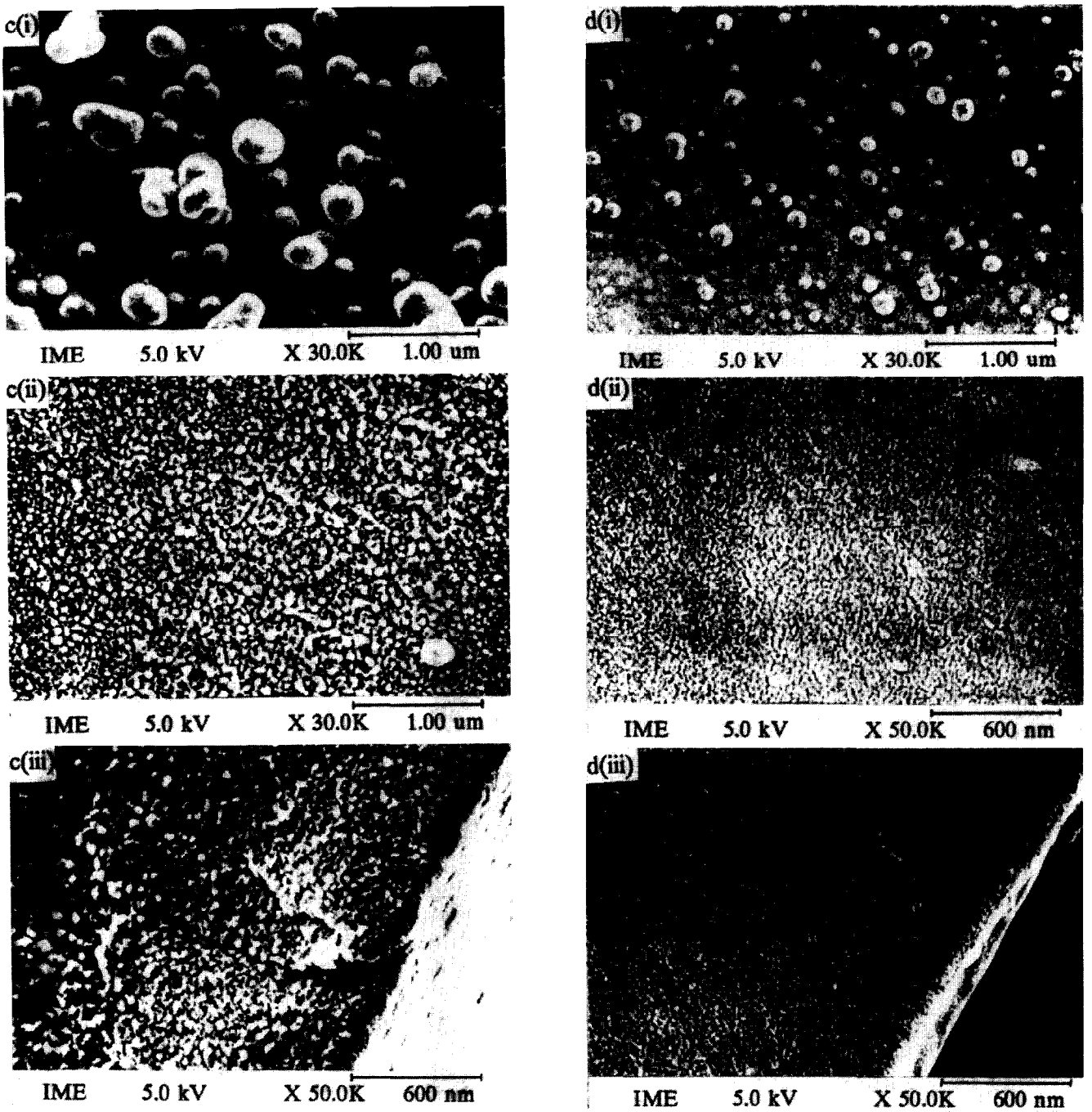

Figure 4 (*Continued*)

into the system to serve the same purpose. In the presence of HEMA which acts as a cosurfactant, a large single-phase region extending from O/W microemulsion to W/O microemulsion, through the intermediate bicontinuous microemulsion, is obtained. This is because with the addition of a cosurfactant, the interpenetration between the surface films of two adjacent droplets increases, thus increasing the coalescence rates, which favours the formation of bicontinuous microemulsions[29]. The smaller microemulsion region obtained for system I using DTAB at aqueous content less than 40 wt% may be due to its larger head group compared to SDS, which makes it unfavourable to form reverse W/O droplet structure. This is in accordance to the surfactant-packing parameter into which a large head group will give rise to a positive curvature[30]. On the other hand, at a higher aqueous content, a slightly larger microemulsion region was obtained for system II, probably due to its monolayer film being of higher flexibility. The persistence length of a film ξ_k is related to its rigidity by[26]

$$\xi_k = a\exp(2\pi K/kT) \qquad (3)$$

where a is the molecular length, K the rigidity constant, k the Boltzmann constant and T the temperature.

At a similar volume fraction (Φ) of oil and water, that is $\Phi_0 = \Phi_w$, ξ_k has been found to be 275 Å for SDS, and 63 Å for DTAB[31,32]. This shows that DTAB has a relatively low rigidity compared to SDS. This may explain why DTAB forms a larger microemulsion region at aqueous contents greater than 40 wt%.

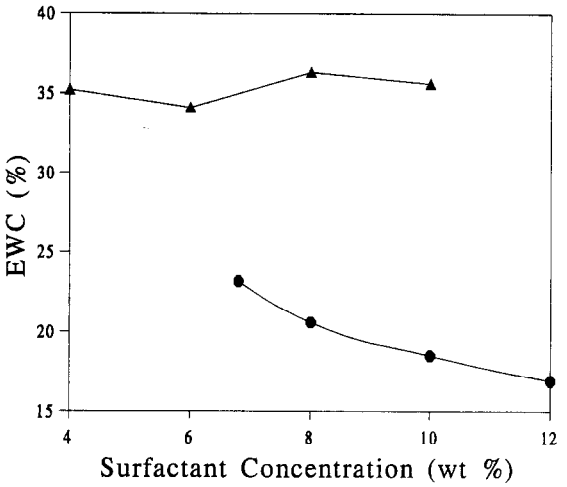

Figure 5 The equilibrium water contents (*EWC*) of the membranes plotted as a function of surfactant concentration made from precursor bicontinuous microemulsions containing MMA/HEMA weight ratio maintained at 30/70 for both SDS and DTAB systems. —▲—, SDS system; —●—, DTAB system

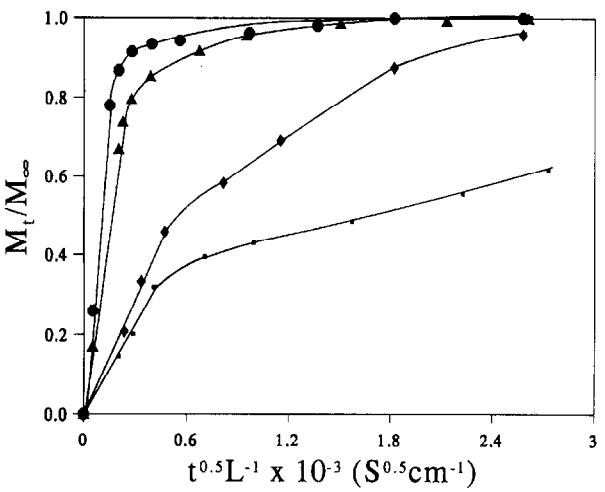

Figure 6 Reduced sorption curves of the membranes S10, S15, S20 and S25 at 25°C. —■—, S10; —◆—, S15; —▲—, S20; —●—, S25

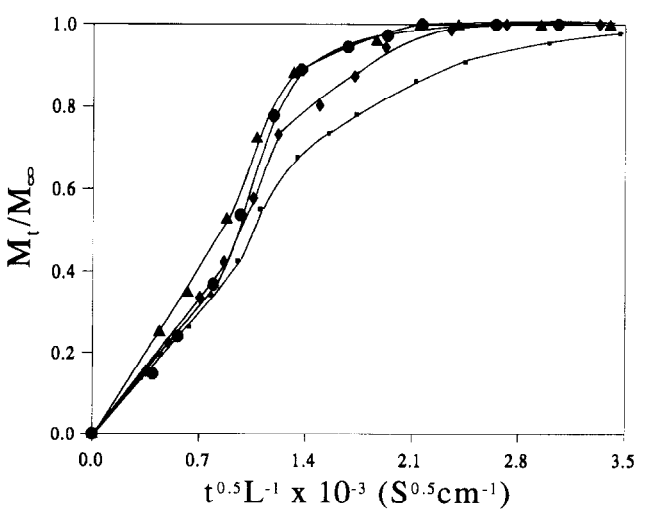

Figure 7 Reduced sorption curves of the membranes D17, D20, D25 and D30 at 25°C. ■, D17; ◆, D20; —▲—, D25; —●—, D30

The higher opacity of the polymeric membranes obtained after polymerization for the SDS system as compared to the DTAB system, indicates that the pore size of the polymeric membranes for the former system was larger than that of the latter. This is evinced from the FESEM observation that the pore size and the size of the aggregates of the system using DTAB were indeed smaller than the system using SDS.

The continuous change of microstructure of the aggregates observed at different concentrations for system I using SDS may be related to its higher persistence length. This allows the formation of elongated or elliptical aggregates, and bigger aggregate size since its film is more rigid. On the contrary, due to the smaller value of ξ_k for DTAB, its interfacial film becomes more flexible and thus leads to the formation of globular aggregates also of smaller size. A decrease in the dimensions of the aggregates with increasing surfactant concentration for SDS and DTAB systems is expected. However, it should be noted here that this decrease of aggregate size is obvious for the SDS system when its concentration is greater than 8 wt%. This is due to the fact that a higher surfactant concentration will stabilize the polymers which are formed in the medium, as has also been observed in our previous study[15]. There is a remarkable difference between SDS and DTAB on the stability of the microemulsion systems after polymerization. Polymeric membranes of higher opacity were obtained for the SDS system compared to the DTAB system, as shown in *Table 1*. This indicates that SDS molecules are less effective in stabilizing the copolymer particles of poly(methyl methacrylate) (PMMA) and poly(2-hydroxyethyl methacrylate) (PHEMA), which may stem from the possibility of a different strength of interaction with the copolymer particles. Much work has been done on the different interaction behaviour of SDS and DTAB towards small molecules or macromolecules[33–35]. It has been found that the interaction of urea or glucose oxidase is greater with DTAB compared to with SDS. Therefore, it is believed that DTAB may possess a higher strength of interaction with copolymer particles of PMMA and PHEMA compared to SDS. This may explain why transparent membranes were obtained for DTAB system.

The higher permeability coefficient obtained at an intermediate surfactant concentration for both systems is probably related to their morphologies. Samples S20 and D25 have interconnected pores or voids extending right from the internal layer and lie close to the skin layer, whereas those samples prepared from low and high surfactant concentrations possess a dense skin layer. Thus, the resistance to water permeability is higher for those membranes containing a dense skin layer. The higher permeability coefficient exhibited by system I using SDS also indicates that the pore size is larger than that of system II using DTAB. These permeability results are supported by the high diffusion coefficients and swelling equilibriums obtained for the SDS system.

A sudden increase in water sorption curves for system II can be explained by its smaller pores, which give rise to a higher capillary action. This is because once water is sorbed into the pores, the capillary forces build up between the wall of the pores and water. With this, the movement of the water molecules accelerated. This phenomenon was not observed in system I because of

the presence of larger pores, whereby capillary action was too small to be detected.

CONCLUSIONS

Control of the pore size of the membranes could be easily effected through the use of surfactants of different nature. From this study, it appears that the pore size of the membranes prepared using SDS is larger as compared to that of DTAB. The higher flexibility of the DTAB monolayer film and its strong interaction with the copolymers of MMA and HEMA may be responsible for its higher stability, which leads to the formation of globular aggregates with smaller pore sizes.

ACKNOWLEDGEMENTS

The authors are grateful to the National University of Singapore for providing financial support under the Research Grant RP 940621/A.

REFERENCES

1 Kesting, R. E. in 'Synthetic Polymeric Membranes: A Structural Perspective', 2nd Edn, Wiley-Interscience, 1985, p. 237
2 Wienk, I. M., van den Boomgaard, Th. and Smolders, C. A. *J. Appl. Polym. Sci.* 1994, **53,** 1011
3 Rukenstein, E. and Sun, F. *J. Appl. Polym. Sci.* 1992, **46,** 1271
4 Rukenstein, E. and Li, H. *Polymer* 1994, **35,** 4343
5 Haque, E., Qutubuddin, S., Benton, S. J. and Fendler, E. J. in 'Polymer Association Structures: Microemulsions and Liquid Crystals' (Ed. M. A. El-Nokaly), ACS Symposium Series No. 384, 1989, p. 64
6 Haque, E. and Qutubuddin, S. *J. Polym. Sci., Polym. Chem. Edn* 1980, **18,** 2641
7 Menger, F. M., Tsuno, T. and Hammond, G. S. *J. Am. Chem. Soc.* 1990, **112,** 1263
8 Menger, F. M., Tsuno, T. and Hammond, G. S. *J. Am. Chem. Soc.* 1990, **112,** 4723
9 Sasthav, M. and Cheung, H. M. *Langmuir* 1991, **7,** 1378
10 Sasthav, M., Palani Raj, W. R. and Cheung, H. M. *Langmuir* 1991, **7,** 2586
11 Palani Raj, W. R., Sasthav, M. and Cheung, H. M. *Langmuir* 1993, **34,** 3305
12 Palani Raj, W. R., Sasthav, M. and Cheung, H. M. *J. Appl. Polym. Sci.* 1993, **47,** 499
13 Gan, L. M., Chieng, T. H., Chew, C. H. and Ng, S. C. *Langmuir* 1994, **10,** 4022
14 Chieng, T. H., Gan, L. M., Chew, C. H. and Ng, S. C. *Polymer* 1995, **36,** 1941
15 Chieng, T. H., Gan, L. M., Chew, C. H., Ng, S. C., Lee, L., Pey, K. L. and Grant, D. *Langmuir* 1995, **11,** 3321
16 Chieng, T. H., Gan, L. M., Chew, C. H., Ng, S. C. and Pey, K. L. *Langmuir* 1996, **12.** 319
17 Burban, J. H., Mengtao, H. and Cussler, E. L. *AIChE J.* 1995, **41,** 907
18 Guo, X. Q., Qiu, K. Y. and Feng, X. D. *Makromol. Chem.* 1990, **191,** 577
19 Spiegler, K. S. *Trans. Faraday Soc* 1958, **54,** 1408
20 Yoshikawa, M., Shiota, A., Sanui, K. and Ogata, N. *New Polym. Mater.*, **1989, 1,** 223
21 Winsor, P. A. *Trans. Faraday Soc.* 1948, **44,** 376
22 Bodet, J. F., Bellare, J. R., Davis, H. T., Scriven, L. E. and Miller, W. G. *J. Phys. Chem.* 1988, **92,** 1898
23 Jahn, W. and Strey, R. *J. Phys. Chem.* 1988, **92,** 2294
24 Talmon, Y. and Prager, S. *Nature* 1977, **1267,** 333
25 Talmon, Y. and Prager, S. *J. Chem. Phys.* 1982, **76,** 1535
26 De Gennes, P. G. and Taupin, C. *J. Phys. Chem.* 1982, **86,** 2294
27 Rogers, C.E. in 'Polymer Permeability' (Ed. J. Comyn), Elsevier, London, 1985, p. 11
28 Leung, R. and Shah, D. O. *J. Colloid Interface Sci.* 1987, **120,** 330
29 Abillon, O., Binks, B. P., Otero, C., Langevin, D. and Ober, R. *J. Phys. Chem.* 1988, **92,** 4411
30 Israelachvili, J. N., Mitchell, D. J. and Ninham, B. W. *J. Chem. Soc., Faraday Trans. II* 1976, **72,** 1525
31 Binks, B. P., Meunier, J., Abillon, O. and Langevin, D. *Langmuir* 1989, **5,** 415
32 Langevin, D. *Acc. Chem. Res.* 1988, **21,** 255
33 Wang, G. and Olofsson, G. *J. Phys. Chem.* 1995, **99,** 5588
34 Moosavi-Movahedi, A. A., Housaindokht, M. R. and Moghaddasi, J. *Thermochim. Acta* 1993, **219,** 143
35 Baglioni, P., Dei, L., Ferroni, E. and Kevan, L. *Progr. Colloid Polym. Sci.* 1991, **84,** 55